MADRID 2015
1-4 June 2015 I IFEMA Madrid

Th N103 13

3D Source Designature Using Source-receiver Symmetry in the Shot Tau-px-py Domain

G. Poole* (CGG), J. Cooper (CGG), S. King (CGG) & P. Wang (CGG)

SUMMARY

While sufficient for many deep water datasets, vertical source designature in shallow water environments can lead to unsatisfactory levels of ringing and amplitude striping, particularly on outer streamers where the assumption of a vertical farfield signature is least accurate. In this paper we modify the tau-px-py Radon equations to introduce a 3D directional designature algorithm. Assuming source-receiver propagation symmetry, a 3D source re-signature operation is introduced and solved with an iteratively re-weighted least squares solver. The results of the strategy lead to improved spatial consistency and a reduction in the level of amplitude striping in the output data. Data examples from a real-world dual-level source project with variable-depth streamers from the North Sea are shown.

Introduction

Marine source designature is an important step in seismic data processing whereby a farfield signature is shaped to a desired wavelet. Historically this operation would relate to debubbling and zero phasing. More recently with the increasing quest for broadband data this process has expanded to include compensation of the source ghost along with gun response shaping.

While source directivity is known to be anisotropic, for example due to the airgun array and free surface ghost, often only vertical designature is applied. Although in many cases the effective directionality of the source array is modest, directional designature can still be an important step for AVO consistent processing (Poole et al. 2013). In deep water settings Lee et al. (2014) perform directional designature by estimating the source take-off angle through analysis of the free surface ghost in the recorded data.

In this paper we consider the source directivity in a shallow water setting. Figure 1a shows a vertical farfield resulting from a dual-level source as in Siliqi et al. (2013). In Figure 1b we see that the application of the vertical designature operator has resulted in a zero phase pulse. Figure 1c analyses the source directivity for the water bottom reflection (100 m depth) across the near channel of 10 streamers with 100 m separation and inline near offset of 150 m as shown by the geometry layout given in Figure 1e. The source signatures highlight a significant change in the effective wavelet with amplitude significantly dropping off to the outer streamers. Figure 1d shows the wavelets for each streamer after vertical designature. While the resulting wavelets for the central cables are reasonable, we still observe more ringing than in the vertical case as the take-off angle here was approximately 37 degrees from vertical. The wavelet at outer cables is much worse, being lower amplitude and not zero-phase as desired.

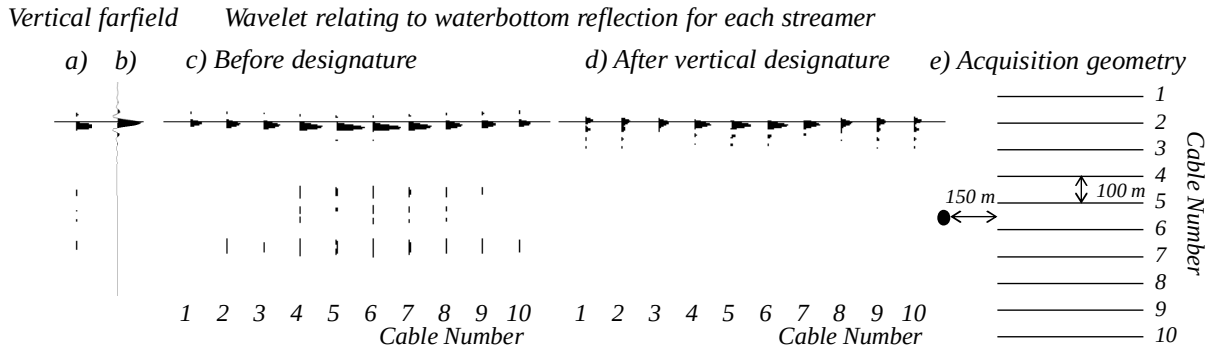

Figure 1 *a) Vertical farfield, b) vertical farfield after designature, c) source signature relating to the waterbottom reflection for each streamer, d) source signature for each streamer after vertical designature, e) schematic of the acquisition geometry.*

In the case of adequate shotpoint coverage 3D directional designature can be applied in the common receiver tau-p_x-p_y domain. In this paper we introduce a 3D directional designature algorithm for towed streamer data applied in the common-shot domain based on source-receiver travel path symmetry.

Theory

Consider the frequency domain definition of the 3D least squares linear Radon transform which may be stated as:

$$d(n) = L(n, m_r)a(m_r) \tag{1}$$

$$L(n, m_r) = e^{-i\omega\tau_r(n,m_r)} \tag{2}$$

$$\tau_r(n, m_r) = o_x(n)p_{rx}(m_r) + o_y(n)p_{ry}(m_r) \tag{3}$$

where ω is the angular frequency, d contains traces from an input shot (index n), and o_x and o_y are the inline and crossline offsets for each input trace. The unknown tau-p_x-p_y representation of the input shot, to be solved by linear inversion, is represented by a. p_{rx} and p_{ry} relate to the slowness of each model trace of a; these are indexed by m_r, with the subscript r relating to receiver side slownesses within the shotpoint gather.

Assuming knowledge of notional source data (preferably derived from nearfield hydrophone data, for example following the approach of Ziolkowski et al. 1982) we may estimate the source farfield signature at any take-off angle through beam forming (Poole et al. 2013):

$$R(m_s) = \sum_{g=1}^{G}\left[N(g)e^{-i\omega\,\tau_s(g,m_s)}\left(e^{i\omega\,\tau_z(g,m_s)} - e^{-i\omega\,\tau_z(g,m_s)}\right)\right] \quad (4)$$

$$\tau_s(g,m_s) = x(g)p_{sx}(m_s) + y(g)p_{sy}(m_s) \quad (5)$$

$$\tau_z(g,m_s) = z(g)p_{sz}(m_s) \quad (6)$$

$$\frac{1}{v_w^2} = p_{sx}^2(m_s) + p_{sy}^2(m_s) + p_{sz}^2(m_s) \quad (7)$$

where N are the notional source data making up an array of G airguns, x and y are the notional source positions relative to the centre of the source, z is the depth of a notional source relative to the sea surface and p_{sx} and p_{sy} relate to the source slowness of each plane wave. The final two exponential terms in Equation (4) relate to the primary and source side ghost, the negative sign before the second of these terms accounting for the free surface reflectivity. p_{sz} is the source slowness derived in the z-direction based on the relation given in Equation (7), where v_w is the water velocity. The subscript s relates to the fact we are now considering source side slownesses.

The farfield signatures from Equation (4) can be used as a basis for source designature in the receiver tau-p domain, where each slowness trace represents a different take-off angle. In the case that source positions are undersampled in at least one direction, for example a towed streamer acquisition, such a formulation is problematic. For this reason we assume symmetry between the source take-off angle and receiver incoming angle as illustrated in Figure 2 (i.e. 1D Earth). By doing this we form a link between source slowness and receiver slowness as given in Equation (8):

$$p_{sx}(m_s) = -p_{rx}(m_r),\ p_{sy}(m_s) = -p_{ry}(m_r) \quad (8)$$

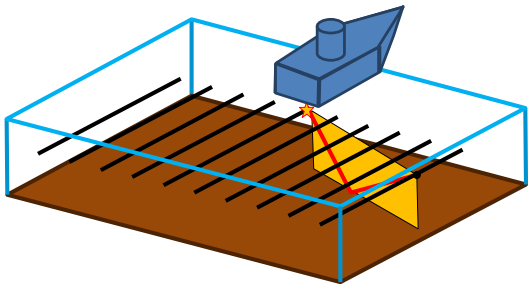

Figure 2 *Geometry of assumed symmetry between source take-off angle and receiver incoming angle.*

Similar to Poole et al. (2013) we combine the operations of re-signature, $R(m_r)$, and reverse tau-p_x-p_y transform, $L(n,m_r)$, as follows:

$$d(n) = L(n,m_r)R(m_r)a_d(m_r) \quad (9)$$

The solution, a_d, to this equation is a tau-p_x-p_y representation of the input shot such that when it is reverse transformed and re-signatured, the input data is reconstructed as accurately as possible. Deriving the model in such a way will ensure that the resulting tau-p_x-p_y transform will be free of source directivity effects (including free surface ghost). To handle the coarse cable spacing the solution is found using an iteratively re-weighted least squares strategy using low frequencies to avoid aliasing at higher frequencies.

Once the transform has been found, it is used to model the source ghost and bubble energy (Figure 3b) which is subtracted from the input data (Figure 3a) to result in combined debubble and deghost (Figure 3c). The process is followed by airgun response shaping which flattens the source array amplitude response as shown in Figures 3 d-e.

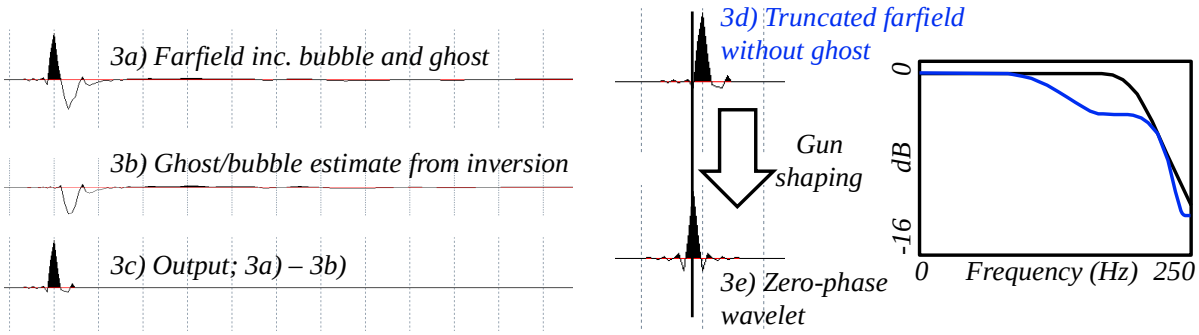

Figure 3 *a)-c) Source deghost and debubble following inversion, d)-e) gun shaping filter.*

While in complex data settings the source-receiver symmetry will break down, in shallow water environments the assumption will be substantially more accurate than only considering vertical take-off. This results in an improved source deghosting and debubble leading to an increase in spatial consistency.

Real data example

The real data example comes from a shallow water North Sea dataset. The acquisition consisted of port and starboard dual-level airgun source arrays with 10 streamers at 100 m separation towed with a variable-depth profile. Figure 4 compares near offset common channels at the waterbottom for outer and inner streamers. While the designature results for the inner streamer are broadly equivalent between vertical and 3D designature, the outer streamer results show a significant reduction in the level of ringing when using the 3D method, as indicated by the arrows.

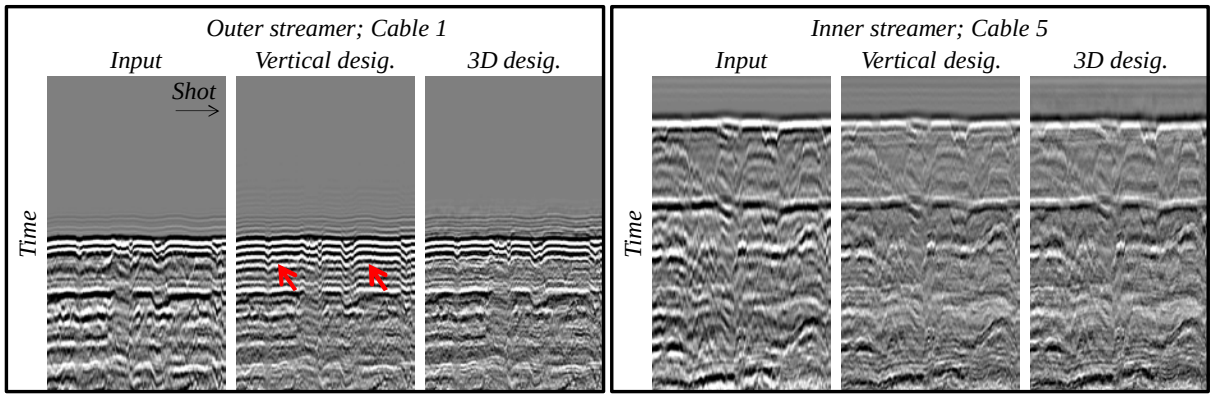

Figure 4 *Near channel designature comparison for outer and inner streamers.*

Figure 5 (left) shows a crossline from a near offset cube after normal moveout (NMO) for input data, after vertical designature, and after 3D designature. The acquisition pattern is evident from the figure, the outer streamers exhibiting an increase in the level of NMO stretch. The vertical designature results show high amplitude ringing in proximity to the waterbottom as shown by the arrows in Figure 5b. The ringing is reduced significantly through the use of 3D designature.

Figure 5 (right) compares an RMS amplitude map calculated in the shallow section for input, vertical designature, and 3D designature as a function of inline and crossline. The displays highlight the reduction in acquisition footprint using 3D designature resulting in a more stationary wavelet.

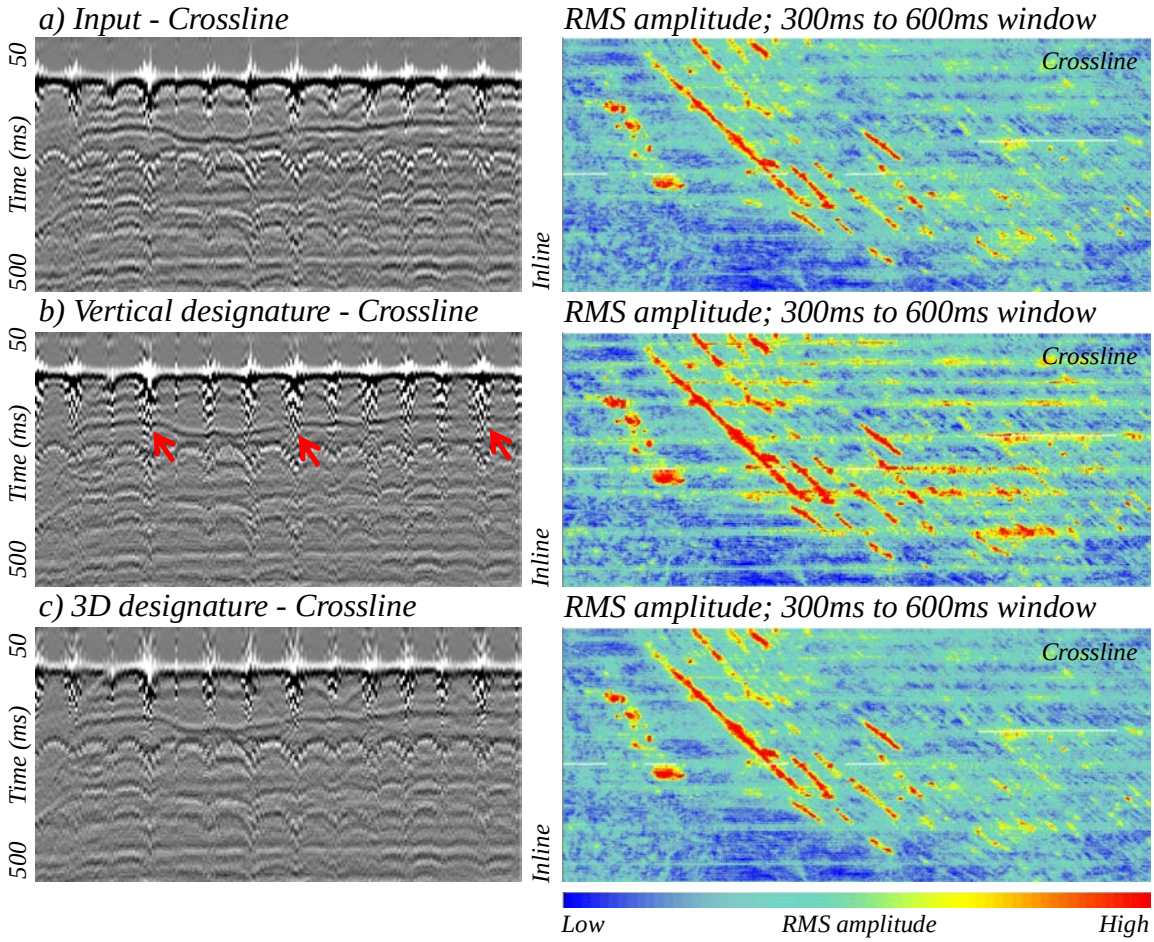

Figure 5 *Designature comparison on near offset cube crosslines (left) and amplitude map QC (right).*

Conclusions

We introduce a 3D shot domain directional designature algorithm assuming source-receiver symmetry. The algorithm is of particular interest for datasets acquired with a wide streamer tow in shallow water environments, which result in strong source directivity effects. The algorithm is based on the linear Radon equations, modified to include a re-signature term. The resulting model represents the data free of source directivity effects and is used to estimate bubble and source ghost energy which is subtracted from the input data. Real data examples highlight the success of this approach for improved wavelet stationarity and a reduction in the acquisition footprint.

Acknowledgements

The authors would like to thank CGG Data Library for the Cornerstone data example. Chris Davison, Tony Wallbank and Sharon Howe are appreciated for help producing the real data example figures.

References

Lee, C-C., Li, Y., Ray, S. and Poole, G. [2014] Directional designature using a bootstrap approach. *84th Annual International Meeting, SEG*, Expanded Abstracts.

Poole, G., Davison, C., Deeds, J., Davies, K. and Hampson, G. [2013] Shot-to-shot directional designature using near-field hydrophone data. *83rd Annual International Meeting, SEG*, Expanded Abstracts.

Siliqi, R., Payen, T., Sablon, R. and Desrues, K. [2013] Synchronized multi-level source, a robust broadband marine solution. *83rd Annual International Meeting, SEG*, Expanded Abstracts.

Ziolkowski, A., Parkes, G.E., Hatton, L. and Haughland, T. [1982] The signature of an air gun array: Computation from near-field measurements including interactions. *Geophysics*, 47, 1413-1421.